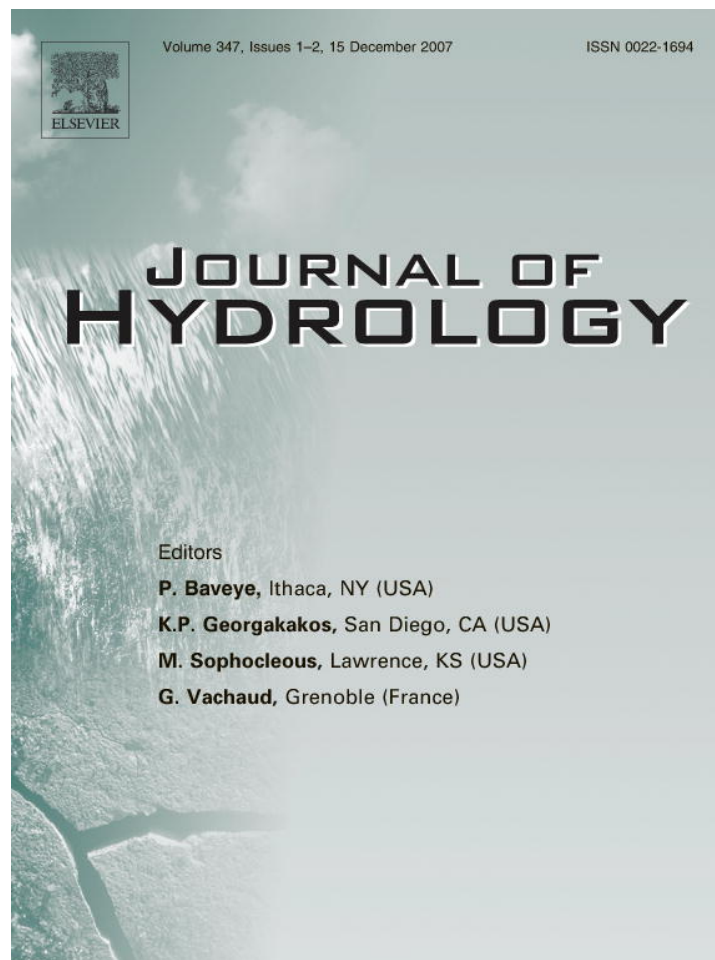


Provided for non-commercial research and education use.  
Not for reproduction, distribution or commercial use.



This article was published in an Elsevier journal. The attached copy is furnished to the author for non-commercial research and education use, including for instruction at the author's institution, sharing with colleagues and providing to institution administration.

Other uses, including reproduction and distribution, or selling or licensing copies, or posting to personal, institutional or third party websites are prohibited.

In most cases authors are permitted to post their version of the article (e.g. in Word or Tex form) to their personal website or institutional repository. Authors requiring further information regarding Elsevier's archiving and manuscript policies are encouraged to visit:

<http://www.elsevier.com/copyright>

available at [www.sciencedirect.com](http://www.sciencedirect.com)journal homepage: [www.elsevier.com/locate/jhydrol](http://www.elsevier.com/locate/jhydrol)

# Analytical estimates of hydraulic parameters for an urbanized estuary – Flushing Bay

Timothy T. Eaton \*

*School of Earth and Environmental Sciences, Queens College–CUNY, 65-30 Kissena Blvd, Flushing, NY 11367, USA*

Received 21 May 2007; received in revised form 21 August 2007; accepted 10 September 2007

## KEYWORDS

Salinity intrusion;  
Dispersion coefficient;  
Groundwater discharge;  
Tidal prism;  
Tidal excursion

**Summary** Prediction of water quality improvements in urban estuaries is an urgent priority for decision making about alternative mitigation measures, especially in the context of changing pollutant loadings and freshwater discharges. Flushing Bay, an embayment of the New York–New Jersey Harbor Estuary, is a “short” estuary (a special class of coastal plain estuary with specific geometric characteristics), in which source loading is changing and little is known about resultant mixing processes and characteristics. First-order values of longitudinal dispersion coefficient, tidal excursion and tidal prism for this estuary have been estimated from non-synoptic salinity data using an adaptation of a one-dimensional theoretical salinity intrusion model. Results indicate that ranges of longitudinal dispersion coefficient are highly dependent on estimates of groundwater discharge, and the spatial distribution of salinity and dispersion coefficient values is most sensitive to conditions at low water slack (LWS). These findings represent a starting point for further investigation of either groundwater discharge to the bay using numerical modeling or field studies of longitudinal dispersion coefficient and mixing using sophisticated tracer methods.

© 2007 Elsevier B.V. All rights reserved.

## Introduction

Water quality is of paramount concern in large urban estuaries where wastewater has been discharged for many decades (Garcia-Barcina et al., 2006; Jeng et al., 2005). Traditional contaminant sources from industrial and urban sewage and stormwater are being reduced due to more stringent regulation. As treatment technologies have improved, the sources and overall quality of water discharging

to these receiving bodies are changing. Numerical simulation of coastal circulation in bays and estuaries is often used to anticipate future trends in water quality, and requires an understanding of the principal hydraulic parameters controlling mixing, such as the coefficient of dispersion, tidal excursion and tidal prism. Although dispersion coefficients can also be estimated using large-scale tracer experiments (Caplow et al., 2003; Ho et al., 2002), these experiments are logistically complex and time consuming. However, the spatial and temporal distribution of salinity in an estuary, even when sampled non-synoptically, contains information on circulation and mixing that can be applied to other

\* Tel.: +1 718 997 3327; fax: +1 718 997 3299.  
E-mail address: [Timothy.Eaton@qc.cuny.edu](mailto:Timothy.Eaton@qc.cuny.edu)

substances in estuarine waters, such as contaminants that degrade water quality.

Here, an adaptation of the theoretical salt intrusion model developed by Savenije (1989, 1993a, 2005) for alluvial estuaries has been applied to salinity data in order to constrain estimates of these parameters for Flushing Bay, an embayment of the New York–New Jersey Harbor Estuary adjacent to New York City (Fig. 1). Since the magnitude of freshwater discharges (in this case, groundwater) to estuaries is linked to the variation in salinity, preliminary discharge values from numerical simulation and field measurement are used to estimate ranges of longitudinal dispersion. Flushing Bay is a one of a particular class of estuary, a “short estuary” similar to that described by Wright et al. (1973) to which this method is not believed to have been applied. The extension of Savenije’s (2005) method described here presents some innovations which may be crucial to understanding the circulation in this type of estuary. Specifically, the cross-sectional area assumed for the shallow Flushing Bay differs significantly between high and low tide, which required a modification of the method. Furthermore, rather than calibrating the model to measurements of salinity at specific equilibrium times during the tidal cycle, the approach used here is to fit envelope curves to the non-synoptic field data. Yet, despite these relaxations of the assumptions of the theoretical framework, the model is shown to be useful for deriving important tidal mixing parameters, demonstrating its robustness.

Flushing Bay discharges into the East River (ER) which separates the island of Manhattan from Long Island, and is

a tidal strait that connects western Long Island Sound (WLIS) to the Atlantic Ocean through New York Harbor. Flushing Bay is the westernmost and historically the most contaminated of several embayments on the north shore of Long Island (Fig. 1). Prior to the 20th century urbanization of the watershed when LaGuardia International Airport was built extending into the bay, it was fed by a stream, Flushing Creek, of which the remnant is now just a narrow extension of the southern end of the Bay. The ER-WLIS system has had a large historical contaminant loading (IEC, 2002) from 18 municipal water pollution control plants (WPCP) and dozens of combined sewage overflow (CSO) discharge points. Flushing Bay has long been the receiving waters for 14 of these CSO outfalls (Fig. 1) from which the fate and transport of CSO particulates has been tracked (Fugate and Chant, 2006) on at least one occasion.

### Hydrologic setting

Nevertheless, the water quality in Flushing Bay is likely to improve considerably over the next few years because of a combination of less wastewater input due to increasing regulation, and more groundwater discharge due to changing water supply and aquifer conditions in the surrounding borough of Queens.

New York City Department of Environmental Protection (NYCDEP) is making major infrastructure investments in large-capacity retention facilities under a consent agreement with the US Environmental Protection Agency to reduce storm event CSO overflows into the NY–NJ Harbor

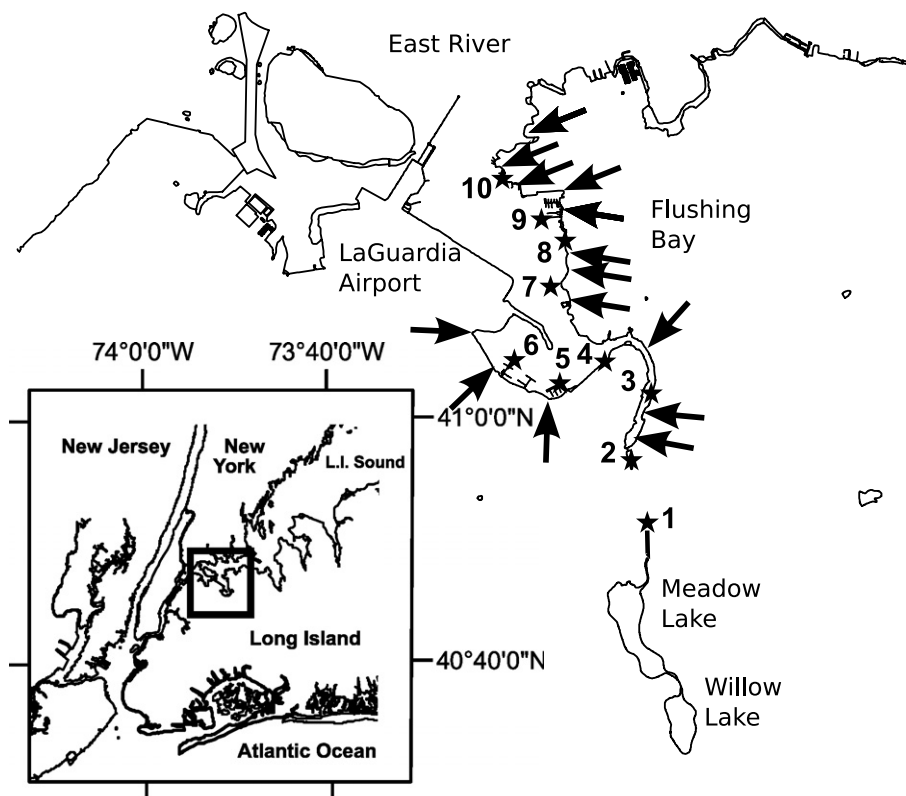


**Figure 1** Location map of Flushing Bay in the New York–New Jersey Harbor Estuary. Numbered stars indicate field sampling sites, and small arrows indicate combined sewage overflow (CSO) discharge points.

Estuary. One of these facilities and associated infrastructure improvements is projected to retain up to 40 million gallons ( $1.5 \times 10^5 \text{ m}^3$ ) of excess CSO discharge at the head of Flushing Bay, and divert it gradually to a WPCP on the East River. This facility has become operational in 2007, thereby reducing the estimated wastewater loading to the Bay by over 40% from previous levels.

Flushing Bay and Creek are of some hydrogeological interest because of the history of groundwater pumping in western Long Island. Municipal water supply for the surrounding borough of Queens was formerly obtained from the Brooklyn-Queens aquifer in the underlying Pleistocene-age un lithified materials. Over the 20th century, hydraulic head was drawn down in this shallow aquifer system, reducing baseflow to major streams, causing many to simply dry up. Flushing Creek was the largest of these streams, and although no flow measurements are known, groundwater flow simulations by the US Geological Survey (USGS) showed that its discharge was probably reduced by about two-thirds (Buxton and Smolensky, 1999; Misut and Monti, 1999). Since the 1980s, municipal water supply has been obtained principally from an aqueduct system bringing surface water from reservoirs in the Catskill mountains north of New York City. Hydraulic head has subsequently been rising, and USGS groundwater modeling simulations have projected a doubling of groundwater discharge to Flushing Creek and Bay by the year 2020 (Buxton and Smolensky, 1999; Misut and Monti, 1999). The combined reduction in CSO discharges and projected increased groundwater input (Fig. 2) represent a major change in source loading to Flushing Bay (Eaton et al., 2006).

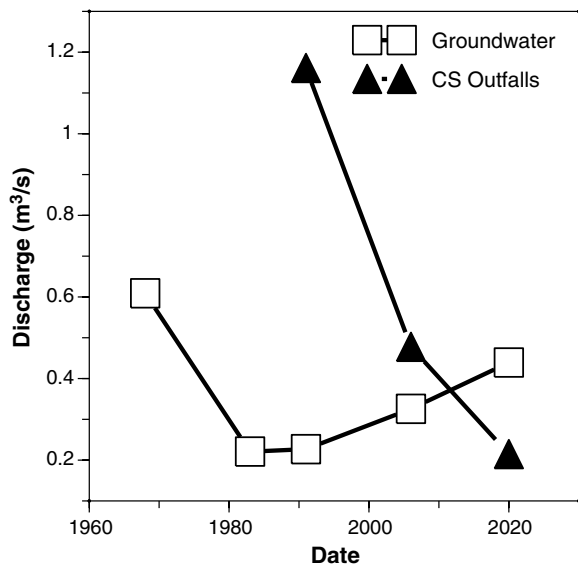


**Figure 2** Changing trends of estimated freshwater discharges to Flushing Creek and Bay: squares indicate estimated and projected groundwater discharge (Buxton and Smolensky, 1999; Misut and Monti, 1999) and solid triangles indicate available and projected CSO annual discharge loadings expressed in comparable units (source: NYCDEP).

### Theoretical background

A comprehensive theoretical framework on the tidal dynamics and salinity intrusion in alluvial estuaries has been presented by Savenije (1986, 1989, 1993a,b,c, 2005). Alluvial estuaries generally resemble “ideal” estuaries defined by their geometry, specifically their flat bottoms and approximately exponential reduction in width and cross-sectional area in a longitudinal direction. This simplification corresponds to the geometry of numerous estuaries worldwide (Savenije, 2005) as well as the Flushing Bay estuary (Fig. 3). However, as opposed to most coastal plain estuaries, the Flushing estuary is a special subcategory of alluvial estuaries called “short” estuaries, limited in length by the topography (Wright et al., 1973). In addition to exponential reduction in longitudinal width and cross-sectional area, “short” estuaries are also characterized by an exponential reduction in depth up-estuary ( $x$ -direction), such that all three parameters can (to first-order) be described as an exponential equation of the form (Savenije, 2005):

$$N = N_0 \exp\left(-\frac{x}{n}\right) \quad (1)$$

In such cases the variables  $N$ ,  $N_0$  and  $n$  can take on values for cross-sectional area ( $A$ ,  $A_0$ ,  $a$ ), width ( $B$ ,  $B_0$ ,  $b$ ) or depth ( $C$ ,  $C_0$ ,  $c$ ) where the convergence lengths  $a$ ,  $b$  and  $c$  ( $x$ -intercepts) are related by  $1/c = (1/a) - (1/b)$ . For Flushing Bay, computed values for area and width parameters are presented later (Table 1). Although the exponential trend for depth could not be verified for this study, the geometry of Flushing Bay corresponds well to this framework (Fig. 3).

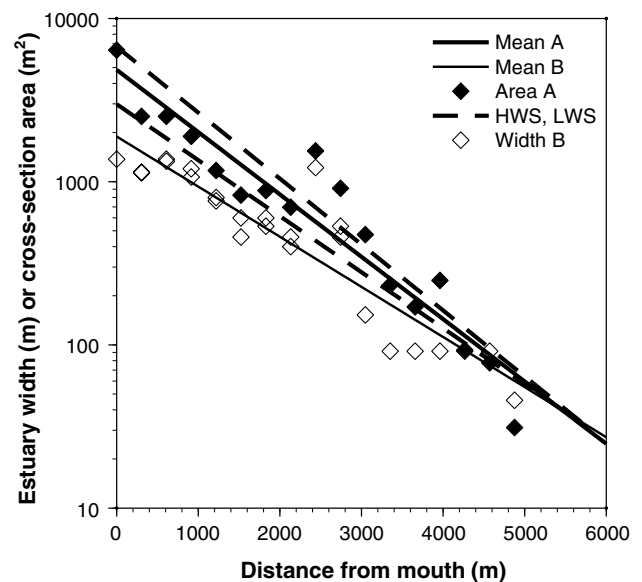


**Figure 3** Verification of approximately exponential variation in tidal cross-sectional area  $A$  and width  $B$  with distance along estuary axis for Flushing Bay. Fitted  $R^2$  values for mean area and width trends are 0.90 and 0.86, respectively. Dashed lines indicate estimated exponential trend of cross-sectional area at high water slack (HWS) and low water slack (LWS) assuming a 2 m tidal range at the mouth of the bay.

**Table 1** Geometrical characteristics and exponential coefficients for Flushing Bay

	Tidal conditions	Exponential coefficients $N_0$ (m <sup>2</sup> or m)	Convergence lengths $n$ (m)	Tidal prism $P$ (10 <sup>6</sup> m <sup>3</sup> )	Calibrated salinities $S_0$ (kg/m <sup>3</sup> )	Calibrated mixing coefficients $\alpha_0$ (m <sup>-1</sup> )
Area A	HWS	$6.7 \times 10^3$	$1.08 \times 10^3$	13.4	28	57
	Mean <sup>a</sup>	$4.8 \times 10^{3b}$	$1.1 \times 10^3$	9.7	—	—
	LWS	$3.0 \times 10^3$	$1.27 \times 10^3$	6.0	22	8
Width B	Mean <sup>a</sup>	$1.9 \times 10^3$	$1.4 \times 10^3$	—	—	—

<sup>a</sup> Mean tidal water levels defined by NOAA on navigation maps.

<sup>b</sup> This is y-intercept of fitted exponential function, actual bay mouth area is  $6.4 \times 10^3$  m<sup>2</sup>.

Note that the convergence (line slopes on Fig. 3) differs between the longitudinal cross-sectional area and the width, which implies a slight bottom slope.

The theory further assumes a small ratio of tidal amplitude to depth, and sufficient mixing laterally, allowing salinity gradients for example, to be considered in one dimension along the axis of the estuary (Horrevoets et al., 2004). One-dimensional analytical solutions to the complete St. Venant hydraulic equations have been developed for different estuarine processes such as tidal propagation, wave celerity and phase lag (Savenije, 2005; Savenije and Veling, 2005). Dispersion processes, both tidal and gravitational, are central to the resultant longitudinal distribution of salinity. Recently, this system of analytical equations was shown to be solvable in closed form when expressed as dimensionless parameters and compared to one-dimensional numerical simulations (Toffolon et al., 2006).

The shape of the measured salt intrusion curve is considered here in an inland direction away from the maximum value  $S_0$  at the estuary mouth. In addition, following Savenije (2005), an empirical relationship is introduced between normalized longitudinal dispersion coefficient  $D/D_0$  and normalized salinity  $S/S_0$  where  $K$  is the dimensionless Van den Burgh's coefficient as follows:

$$\frac{D}{D_0} = \left(\frac{S}{S_0}\right)^K \quad (2)$$

The unsteady-state one-dimensional salt balance equation presented by Savenije (2005) is

$$r_s A \frac{\partial S}{\partial t} + (Q_t + Q_f) \frac{\partial S}{\partial x} - \frac{\partial}{\partial x} \left( A D \frac{\partial S}{\partial x} \right) = -S R_s \quad (3)$$

where  $r_s$  is the storage width ratio between entire wetted surface and flow width (–).

$S = S(x, t)$  is the salinity in kg/m<sup>3</sup>,  $A = A_0 \exp(-\frac{x}{a})$  is the cross-sectional area of the estuary (m<sup>2</sup>),  $Q = Q(x, t)$  is the discharge, divided into tidal ( $Q_t$ ) and freshwater ( $Q_f$ ) parts (m<sup>3</sup>/s),  $D = D(x, t)$  is the longitudinal dispersion coefficient (m<sup>2</sup>/s), and  $R_s$  is the salinity source term (m<sup>2</sup>/s).

Simplifying to tidal average (TA) conditions following first-order approximations used by other workers (Fischer et al., 1979; O'Kane, 1980), and assuming equilibrium between advective and dispersive terms, Savenije (2005) integrated this salt balance equation with respect to  $x$  to give

$$Q_f(S_{TA} - S_f) - A_{TA} D_{TA} \frac{\partial S_{TA}}{\partial x} = 0 \quad (4)$$

with boundary conditions  $S_{TA} = S_f$  and  $\partial S_{TA} / \partial x = 0$  as  $x \rightarrow \infty$ .

Two other cases besides tidal average (TA) where this equation is applicable are high water slack (HWS) and low water slack (LWS), which are of greater interest here because they provide envelope curves for values of the longitudinal salinity distribution. The curves differ merely by a horizontal translation in  $S$ – $x$  space equal to half the tidal excursion. For the two equilibrium conditions at HWS and LWS, the resulting solutions have been shown to accurately predict longitudinal salinity distributions at numerous alluvial estuaries worldwide (Savenije, 2005), even when the estuary is multi-channeled (Nguyen and Savenije, 2006). Assuming the salinity  $S_f$  of freshwater inflow is zero and the subscript  $i$  corresponds to either HWS or LWS, the equation expressed in general form is as follows:

$$\frac{\partial S_i}{\partial x} = \frac{Q_f}{A_i D_i} (S_i) \quad (5)$$

If  $Q_f / (A_i D_i)$  were constant (which is seldom the case), this would have the well-known solution with salinity at the estuary mouth  $S_0$

$$S_i(x) = S_0 \exp\left(\frac{Q_f}{A_i D_i} x\right) \quad (6)$$

However, differentiation of Eq. (2) with respect to  $x$  as shown by Savenije (1993a, 2005) gives the expression for the distribution of longitudinal dispersion with distance

$$\frac{dD_i}{dx} = K \frac{D}{S} \frac{\partial S}{\partial x} \quad (7)$$

The right-hand side of the above equation is equivalent to  $K(Q_f/A)$ , based on elaboration of the Van den Burgh's equation (Eq. (2)). Furthermore, taking into account the exponential geometry (Eq. (1)), particularly the cross-sectional area of the estuary, the solution for longitudinal dispersion (Savenije, 2005) is

$$D = D_0 + \frac{K a Q_f}{A_0} \exp\left(\frac{x}{a} - 1\right) \quad (8)$$

where  $a$  is the cross-sectional convergence length (m).

## Methods

The difficulty with using Eqs. (8), (6) and (2) to estimate the distribution of longitudinal dispersion coefficient  $D$  is that the value of freshwater discharge ( $Q_f$ ) is often not well-known, as in the case of Flushing Bay. Savenije (1989) presented a spreadsheet method of solution in which a new variable is introduced

$$\alpha_0 = D_i/Q_f \quad (9)$$

This variable  $\alpha_0$ , considered a mixing coefficient (Nguyen and Savenije, 2006) at the estuary mouth, can be substituted into Eq. (6), allowing different values of  $\alpha_0$  to be tested against salinity measurements. In this way, the bounding HWS and LWS salinity curves (Eq. (5)) can be fitted to salinity data by trial and error.

An adaptation of the spreadsheet method (Savenije, 1989) was employed here in which some of the assumptions in the theoretical development could be relaxed. First, in contrast to normal marine salinity, the salinity at the mouth of Flushing Bay is not constant because the East River itself forms part of the larger NY–NJ Harbor Estuary. So two different values each of  $S_0$  and  $\alpha_0$  were identified, allowing independent fitting of the HWS and LWS curves to the dataset. Dispersion coefficients and values of mixing coefficient  $\alpha_0$  vary with the tidal stage, but the Van den Burgh coefficient  $K$  should be constant for any given estuary (Savenije, 2005). The tidal excursion  $E_0$  was also assumed to be constant for the period of this study in 2006, allowing the tidal prism  $P$  to be estimated as the product of  $E_0$  and estuary mouth area for HWS and LWS conditions. Secondly, the magnitude of the cross-sectional area of the bay varies considerably because of the tidal range of approximately 2 m. The depth at the mouth was assumed to be 1 m higher than the mean at high tide (HWS) and 1 m lower than the mean at low tide (LWS). Hence, the resulting cross-sectional area of Flushing Bay at its mouth ( $A_0$ ) is much larger at high tide than at low-tide (Fig. 3) because most of the bay is shallow (<2 m depth) around the dredged narrow shipping channel (>4 m depth) along the axis. Two different exponential functions (HWS and LWS) of the form of Eq. (1) were used here to describe the variation of area along the estuary axis rather than one single (TA) function (Savenije, 1989; Savenije, 2005). Coefficients and convergence lengths for these exponential functions were computed.

Salinity data were collected once weekly at each of ten sites around Flushing Bay (Fig. 1) during the summer of 2006 (Eaton et al., 2006) using an Extech portable refractometer Model 99716. This watershed has been considerably transformed by urbanization, and the meanders of the former Flushing Creek were replaced in the early 20th century by two connected artificial basins, Meadow Lake and Willow Lake. They have a hydraulic connection to the narrow southern extension of Flushing Bay through a culvert and channel extending north from Meadow Lake. Site 1 was located where the channel enters this culvert. In Flushing Bay proper, data collection was limited to shoreline locations, but many sites had long piers that extended out into the bay. Since this shallow embayment is well mixed laterally and vertically (Fugate and Chant, 2006), it was assumed that these data are representative of the average values in cross-sections on the longitudinal profile. The sampling schedule was designed to provide several measurements at high, midrange and low tidal stages for each site. There is no tidal gage in Flushing Bay, so the approximate relative tidal level was estimated when data were collected, and checked against records from the nearest National Oceanic and Atmospheric Administration (NOAA) tidal gage in the East River.

In this paper, envelope curves defined by Eq. (6) are fit to field measurements to constrain values of the dispersion

coefficient and tidal excursion in the Flushing Bay estuary. A sensitivity analysis is applied to these data, then ranges of longitudinal dispersion coefficient are presented based on independent estimates of freshwater input. Freshwater input is a combination of direct groundwater discharge and surface water discharge through the culvert and channel from Meadow Lake, however it all originates from groundwater since there are no significant surface inflows to Meadow or Willow Lakes. It is also assumed that the influence of this continuous discharge on salinity variation in Flushing Bay predominates the infrequent episodic discharges from CSO discharges during storm events. To constrain ranges of dispersion coefficient  $D_i$ , steady-state estimated high, midrange and low values of freshwater input ( $Q_f$ ) were obtained from three independent sources. The first was a preliminary groundwater flow model calibrated to measured water level elevations in monitoring wells (Busciolano, 2001), the second a USGS estimate from more sophisticated groundwater flow modeling for the year 1991 (Misut and Monti, 1999), and lastly a 2006 field measurement of discharge using the standard velocity–area method along the channel leading north from Meadow Lake during low-tide conditions. While it is likely that groundwater discharge to the lakes and Flushing Bay varies temporally with the tidal cycle, and the distribution of groundwater discharge varies spatially along the axis of the estuary, perhaps according to an exponential or similar function (Bokuniewicz, 1992), analysis at that level of detail was beyond the scope of this study.

## Results

Measurement values of salinity with distance from the mouth of Flushing Bay along with the fitted HWS and LWS envelope curves (Fig. 4) show that the salinity intrusion curve is dome-shaped, which is typical for a tidally dominated estuary with a wide mouth and relatively low freshwater discharge (Savenije, 1993a, 2005). Near the mouth of the bay, the salinity gradient is very low with salinity values from about 22 to 28 kg/m<sup>3</sup>, consistent with values reported from the East River (Sweeney and Sanudo-Wilhelmy, 2004). As the salinity gradient increases inland, this range expands, to almost 0–15 kg/m<sup>3</sup> at the landward end (Site 1, 5791 m). Most of the data values near the upper HWS curve represent high tide conditions, whereas many of the values nearest the lower LWS curve represent low-tide conditions. Discrepancies in this pattern can be attributed to the uncertainty in tidal stage at each location and delayed mixing at the shoreline sampling locations. Of course, most of the data represents tidal level at some intermediate stage, and few extreme values of tide stage and salinity could be sampled. Tidal excursion cannot be interpreted directly from the horizontal distance between the HWS and LWS curves as in the original spreadsheet model (Savenije, 1989), because the HWS and LWS salinity intrusion is calculated independently. However, the tidal excursion is estimated to be 2000 m based on the calculated relationship between the tidal average (TA) curve and the HWS curve following Savenije (1989). Estimated tidal prism and coefficients for the exponential equations used to represent the longitudinal variation in

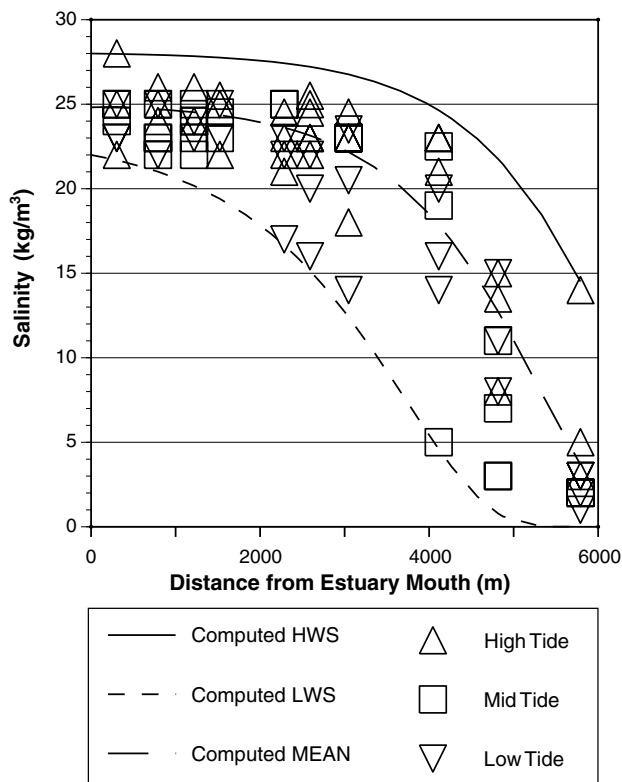


**Figure 4** Calculated salinity intrusion curves fitted to data collected in Flushing Bay. The upper curve corresponds to conditions at high water slack (HWS) and the lower curve corresponds to low water slack (LWS). Field data values were collected at all different stages of the tide, hence they fall within the envelope curves.

estuary cross-sectional area, width and fitted salinity intrusion curves are presented in Table 1.

The value for the Van den Burgh coefficient  $K$  which is characteristic of alluvial estuaries (Eq. (2)) is estimated at 0.2–0.25 for Flushing Bay, based on calibration of this model: that is, simultaneous fitting of the HWS and LWS salinity envelope curves (Fig. 4) to the field data. This low value of  $K$  is typical of estuaries where tidally driven mixing is more important than density-driven mixing. A sensitivity analysis (Fig. 5) was conducted by varying the value of  $K$  within reasonable ranges ( $0 < K < 1$ ). The major effect of varying the value of the Van den Burgh coefficient is to cause a steeper salinity gradient inland for the HWS curve and especially for the LWS curve at high values of  $K$  ( $>0.9$ ). The sensitivity analysis confirms that 0.2–0.25 is a reasonable estimate for  $K$ , however, the solutions are not sensitive enough and the non-synoptic data set is not large enough to refine this estimate any further.

The fitted envelope curves for HWS and LWS are much more sensitive to values of the mixing coefficient  $\alpha_0$  for each condition. Salinity intrusion curves were calculated for each of the values of  $\alpha_0$  that caused significant differences in the shapes of the curves (Fig. 6). The LWS curve varies more depending on the value of the mixing coefficient ( $\alpha_0 \pm 4$ ) for the data collected in this study than does the HWS curve ( $\alpha_0 \pm 24$ ). Of course, the location of

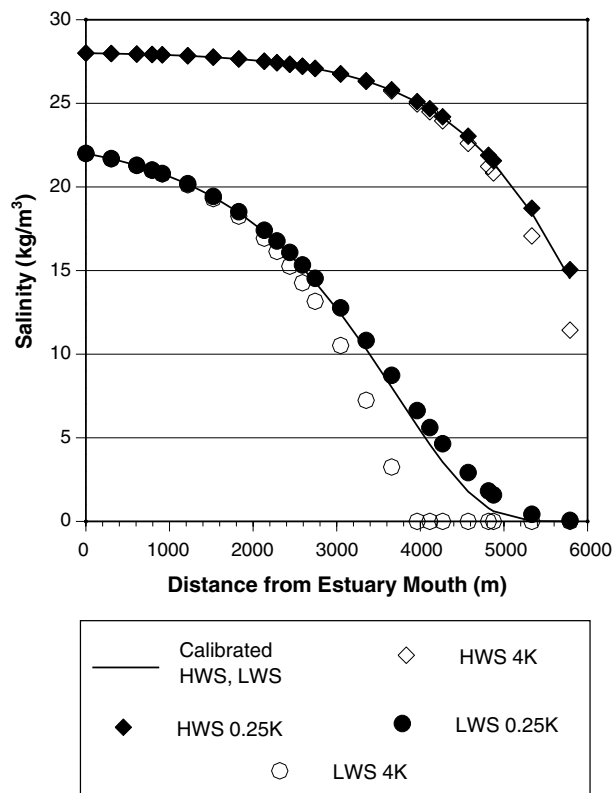


**Figure 5** Sensitivity of calculated salinity intrusion curves to the value of the van den Burgh coefficient  $K$ . Points indicate shape of intrusion curves for selected multiples of  $K$  as shown.

the steepest portion of the salinity gradient shifts in the estuary with the tides, but data were not collected further up into the estuary in Meadow and Willow Lakes. The HWS curve is most sensitive to values of  $\alpha_0$  near the toe of the salinity intrusion whereas the LWS curve is most sensitive in the middle reaches of the estuary. Therefore, over most of the estuary length, when salinity measurements at LWS are used in conjunction with this modified model, LWS estimates of  $\alpha_0$  and  $D_0$  are likely to be more accurate than HWS estimates of these parameters using HWS salinity data.

The sensitivity of the salinity intrusion curves at HWS and LWS also translates into a sensitivity of the dispersion coefficient  $D$  to the mixing coefficient  $\alpha_0$ . The normalized longitudinal dispersion curves calculated with Eq. (2) (Fig. 7) indicate that at LWS, the dispersion coefficient is increasingly sensitive inland to the mixing coefficient until it becomes zero where freshwater dominates, as predicted by the theoretical framework (Savenije, 2005). In contrast, the calibrated exponential function for dispersion only shows an inland decrease to approximately 86% of the dispersion coefficient value at the mouth of the bay for HWS conditions, and is much less sensitive to values of mixing coefficient  $\alpha_0$ .

Estimated values of the longitudinal dispersion coefficient  $D_0$  at the mouth of Flushing Bay for different values of mixing coefficient  $\alpha_0$  and freshwater input are shown in Table 2. The ranges of dispersion coefficient values corresponding to the calibrated values of  $\alpha_0$  are rather broad for HWS:  $9 \text{ m}^2 \text{ s}^{-1}$  to  $26 \text{ m}^2 \text{ s}^{-1}$  but considerably narrower

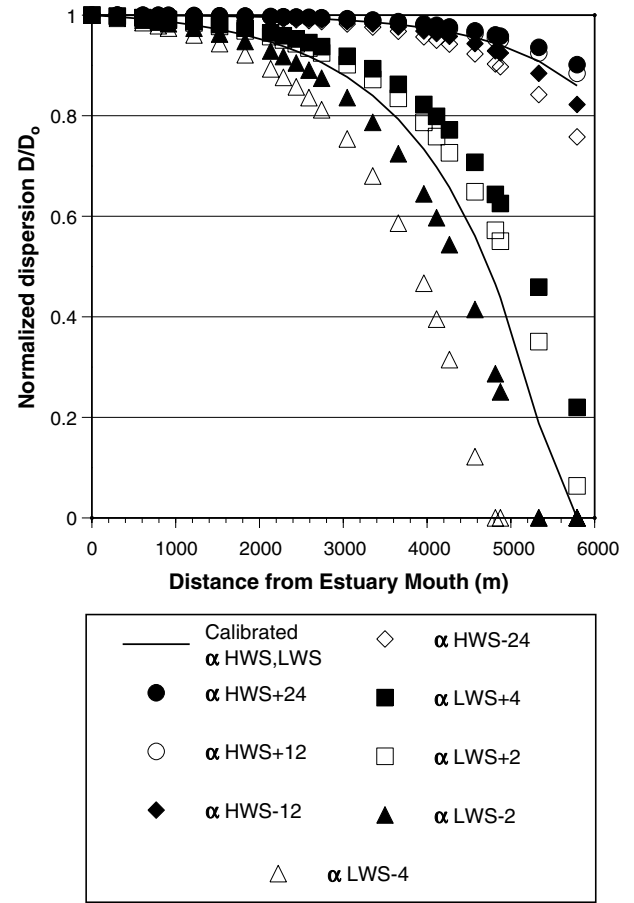
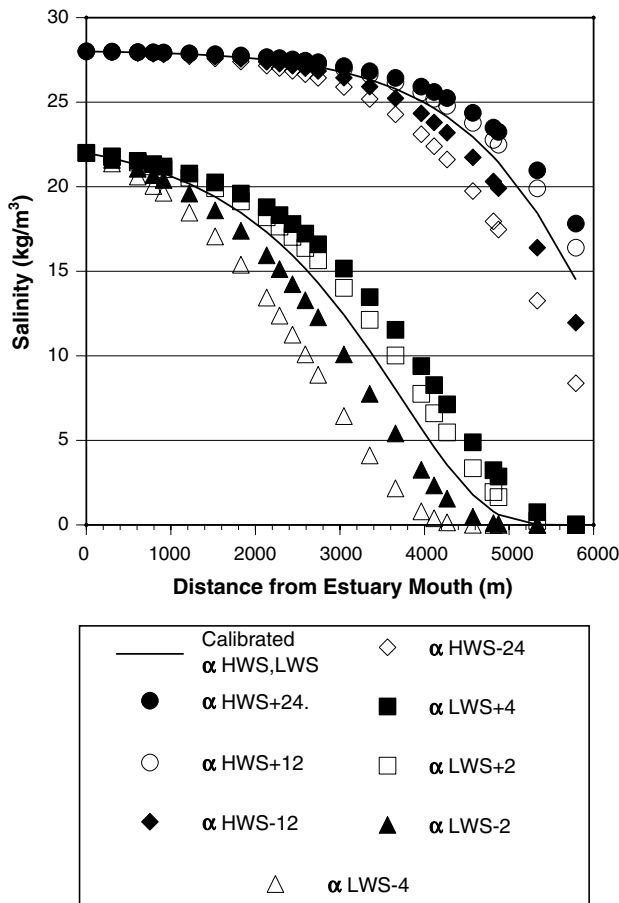


**Figure 6** Sensitivity of calculated salinity intrusion curves to values of mixing coefficient  $\alpha_0$  for both high water slack (HWS) and low water slack (LWS) conditions. Points indicate shape of intrusion curves for selected variation in  $\alpha_0$  as shown.

**Figure 7** Sensitivity of calculated dimensionless dispersion curve to values of mixing coefficient  $\alpha_0$  for both high water slack (HWS) and low water slack (LWS) conditions. Points indicate shape of dispersion curves for selected variation in  $\alpha_0$  as shown.

for LWS:  $1\text{--}4\text{ m}^2\text{ s}^{-1}$ , and these values would decline exponentially inland according to the curves in Fig. 7. However, in the absence of field experiments, they represent first-order estimates of the magnitude of this important mixing parameter. They compare favorably to actual values of longitudinal dispersion coefficient of approximately  $70\text{ m}^2\text{ s}^{-1}$  determined from  $\text{SF}_6$  tracer experiments in the nearby Hudson River (Ho et al., 2002), in which advective flow due to river discharge as well as tidal forcing is much greater.

Considering the uncertainty of freshwater inflow to Flushing Bay, and the approximations involved in estimating these values from the one-dimensional theoretical framework using non-synoptic field data, these data provide an important starting point for additional characterization of mixing processes in this urbanized estuary, in which little other field data is available. For example, future tracer experiments using  $\text{SF}_6$  could be used to verify and perhaps

**Table 2** Sensitivity and estimated ranges of longitudinal dispersion coefficients at mouth of Flushing Bay calculated from Eq. (9)

Tidal stage	Mixing coefficient $\alpha_0$ ( $\text{m}^{-1}$ ) range	Estimated freshwater inflow $Q_f^a$ ( $\text{m}^3/\text{s}$ )		
		0.163	0.227	0.453
		Dispersion coefficients $D_0$ ( $\text{m}^2/\text{s}$ )		
HWS conditions	Max: $\alpha_0 + 24$	13.2	18.3	36.7
	Calibrated $\alpha_0$	9.31	12.9	25.8
	Min: $\alpha_0 - 24$	5.39	7.47	14.9
LWS conditions	Max: $\alpha_0 + 4$	1.96	2.72	5.44
	Calibrated $\alpha_0$	1.31	1.81	3.62
	Min: $\alpha_0 - 4$	0.65	0.91	1.81

<sup>a</sup> As described in text.

refine these values and thereby constrain values of freshwater (groundwater) discharge to the Bay using the relationships described herein. Since groundwater discharge has been projected to increase substantially (Buxton and Smolensky, 1999; Misut and Monti, 1999), these findings and methods can provide important independent verification of numerical flow modeling predictions. Conversely, if more refined numerical modeling (taking into account density differences for example) or detailed field measurements (using temperature or automated seepage measurement devices) provide new data on groundwater discharge, values of longitudinal dispersion coefficient in Flushing Bay can be further constrained.

## Conclusions

First-order values of longitudinal dispersion coefficient, tidal excursion and tidal prism for Flushing Bay have been estimated from non-synoptic salinity data using an adaptation of a one-dimensional theoretical salinity intrusion model (Savenije, 2005). Since the pollutant loadings and sources of freshwater discharge to this embayment of the NY–NJ Harbor Estuary are changing rapidly due to a combination of stricter CSO discharge regulation and water supply dynamics, these data are a starting point for additional investigation of future water quality improvements. The relationships between freshwater (groundwater) discharge to Flushing Bay and estimates of dispersion coefficient outlined here provide a mechanism for independent verification of either better groundwater discharge estimates or better dispersion coefficient estimates determined from field tracer studies.

The relaxation of some of the assumptions of the underlying theory, and the extension of the salinity intrusion model used here suggests that the model is quite robust. Nevertheless, as suggested by Savenije (2005), a better way of collecting salinity data to apply this model would be along the estuary axis from a moving boat following the tide at HWS and LWS. In cases similar to this study, where such a protocol was not feasible, this work shows that the adapted salinity intrusion model can still be useful for estimating tidal and mixing parameters by fitting envelope curves to non-synoptic data. If such HWS and LWS data can also be collected from a moving boat, the comparison of such synoptic and non-synoptic data, in conjunction with the salinity model results, could illuminate aspects of estuarine circulation which may be specific to this type of “short” estuary, a subset of the general class of alluvial estuaries.

To date, efforts at predicting water quality changes and residence time in Flushing Bay using numerical coastal circulation models have been hampered because the effect of groundwater discharge to the Bay has apparently not been considered (source: NYCDEP Flushing Bay stakeholders public meetings 2006, 2007). In particular, public policy decisions about the advisability of removing control structures such as a breakwater extending into the bay (Fig. 1) depend on a better understanding of mixing processes in this urbanized estuary. The reliability of numerical modeling of residence time and water circulation in Flushing Bay and other similar urbanized estuaries depends on robust in-

put parameters. The values of longitudinal dispersion coefficient, tidal excursion and tidal prism estimated in this paper represent a first step in that direction.

## Acknowledgements

The assistance of George Hendrey in collecting channel velocity–area discharge data and Jay Bobbins and Sucharit Dutta in collecting salinity data is greatly appreciated. The comments of two anonymous reviewers helped to improve the manuscript considerably. This work was funded in part by the City University of New York (NNYN/CUNY Program for Ecological/Environmental Research (PEER) in New York).

## References

- Bokuniewicz, H.J., 1992. Analytical descriptions of subaqueous groundwater seepage. *Estuaries* 15 (4), 458–464.
- Busciolano, R., 2001. Water-table and potentiometric-surface altitudes of the Upper Glacial, Magothy, and Lloyd Aquifers on Long Island, New York, in March–April 2000, with a summary of hydrogeologic conditions. Water-Resources Investigations Report 01-4165, US Geological Survey, Coram.
- Buxton, H.T., Smolensky, D.A., 1999. Simulation of the effects of development of the ground-water flow system of Long Island, New York. Water-Resources Investigations Report 98-4069, US Geological Survey, Coram.
- Caplow, T., Schlosser, P., Ho, D.T., Santella, N., 2003. Transport dynamics in a sheltered estuary and connecting tidal straits: SF6 tracer study in New York Harbor. *Environmental Science and Technology* 37 (22), 5116–5126.
- Eaton, T.T., Zheng, Y., Bobbins, J., Dutta, S., 2006. Hydrology and water quality in a heavily urbanized estuary. *GSA Abstracts with Programs* 38 (7).
- Fischer, H.B., List, E.J., Koh, R.C.Y., Imberger, J., Brooks, N.H., 1979. *Mixing in Inland and Coastal Waters*. Academic Press, New York.
- Fugate, D., Chant, B., 2006. Aggregate settling velocity of combined sewage overflow. *Marine Pollution Bulletin* 52 (4), 427–432.
- Garcia-Barcina, J.M., Gonzalez-Oreja, J.A., De la Sota, A., 2006. Assessing the improvement of the Bilbao estuary water quality in response to pollution abatement measures. *Water Research* 40 (5), 951–960.
- Ho, D.T., Schlosser, P., Caplow, T., 2002. Determination of longitudinal dispersion coefficient and net advection in the tidal Hudson River with a large-scale, high resolution SF6 tracer release experiment. *Environmental Science and Technology* 36 (15), 3234–3241.
- Horrevoets, A.C., Savenije, H.H.G., Schuurman, J.N., Graas, S., 2004. The influence of river discharge on tidal damping in alluvial estuaries. *Journal of Hydrology* 294 (4), 213–228.
- IEC, 2002. *The Year of Clean Water: Commemorating the 30th Anniversary of the Clean Water Act*, Interstate Environmental Commission, New York.
- Jeng, H.A.C., Englands, A.J., Bakeer, R.M., Bradford, H.B., 2005. Impact of urban stormwater runoff on estuarine environmental quality. *Estuarine Coastal and Shelf Science* 63 (4), 513–526.
- Misut, P.E., Monti, J., 1999. Simulation of ground water flow and pumpage in King and Queens Counties, Long Island, New York. Water-Resources Investigations Report 98-4071, US Geological Survey, Coram.

- Nguyen, A.D., Savenije, H.H.G., 2006. Salt intrusion in multi-channel estuaries: a case study in the Mekong Delta, Vietnam. *Hydrology and Earth System Sciences* 10 (5), 743–754.
- O’Kane, J.P., 1980. *Estuarine Water Quality Management*. Pitman Publishing Ltd., London, UK.
- Savenije, H.H.G., 1986. A One-Dimensional Model for Salinity Intrusion in Alluvial Estuaries. *Journal of Hydrology* 85 (1–2), 87–109.
- Savenije, H.H.G., 1989. Salt Intrusion Model for High-Water Slack, Low-Water Slack, and Mean Tide on Spread Sheet. *Journal of Hydrology* 107 (1–4), 9–18.
- Savenije, H.H.G., 1993b. Determination of Estuary Parameters on Basis of Lagrangian Analysis. *Journal of Hydraulic Engineering-ASCE* 119 (5), 628–642.
- Savenije, H.H.G., 1993a. Composition and driving mechanisms of longitudinal tidal average salinity dispersion in estuaries. *Journal of Hydrology* 144 (1–4), 127–141.
- Savenije, H.H.G., 1993c. Predictive model for salt intrusion in estuaries. *Journal of Hydrology* 148 (1–4), 203–218.
- Savenije, H.H.G., 2005. *Salinity and Tides in Alluvial Estuaries*. Elsevier, Amsterdam, pp. 194.
- Savenije, H.H.G., Veling, E.J.M., 2005. Relation between tidal damping and wave celerity in estuaries. *Journal of Geophysical Research – Oceans* 110 (C4).
- Sweeney, A., Sanudo-Wilhelmy, S.A., 2004. Dissolved metal contamination in the East River-Long Island sound system: potential biological effects. *Marine Pollution Bulletin* 48 (7–8), 663–670.
- Toffolon, M., Vignoli, G., Tubino, M., 2006. Relevant parameters and finite amplitude effects in estuarine hydrodynamics. *Journal of Geophysical Research – Oceans* 111 (C10).
- Wright, L.D., Coleman, J.M., Thom, B.G., 1973. Processes of channel development in a high-tide range environment: Cambridge Gulf-Ord river delta, Western Australia. *Journal of Geology* 81, 15–41.